

Review

Real-Time Identification of Oxygen Vacancy Centers in LiNbO_3 and SrTiO_3 during Irradiation with High Energy Particles

Miguel L. Crespillo ^{1,2,*} , Joseph T. Graham ³, Fernando Agulló-López ², Yanwen Zhang ⁴ 
and William J. Weber ^{1,4,*} 

¹ Department of Materials Science and Engineering, University of Tennessee, Knoxville, TN 37996, USA

² Centro de Microanálisis de Materiales, CMAM-UAM, Cantoblanco, 28049 Madrid, Spain; fal@uam.es

³ Department of Nuclear Engineering and Radiation Science, Missouri University of Science and Technology, Rolla, MO 65409, USA; grahamjose@mst.edu

⁴ Oak Ridge National Laboratory, Materials Science and Technology Division, Oak Ridge, TN 37831, USA; zhangy@ornl.gov

* Correspondence: mcrespil@utk.edu (M.L.C.); wjweber@utk.edu (W.J.W.);
Tel.: +1-865-360-2287(M.L.C.); +1-865-974-0415 (W.J.W.)

Abstract: Oxygen vacancies are known to play a central role in the optoelectronic properties of oxide perovskites. A detailed description of the exact mechanisms by which oxygen vacancies govern such properties, however, is still quite incomplete. The unambiguous identification of oxygen vacancies has been a subject of intense discussion. Interest in oxygen vacancies is not purely academic. Precise control of oxygen vacancies has potential technological benefits in optoelectronic devices. In this review paper, we focus our attention on the generation of oxygen vacancies by irradiation with high energy particles. Irradiation constitutes an efficient and reliable strategy to introduce, monitor, and characterize oxygen vacancies. Unfortunately, this technique has been underexploited despite its demonstrated advantages. This review revisits the main experimental results that have been obtained for oxygen vacancy centers (a) under high energy electron irradiation (100 keV–1 MeV) in LiNbO_3 , and (b) during irradiation with high-energy heavy (1–20 MeV) ions in SrTiO_3 . In both cases, the experiments have used real-time and in situ optical detection. Moreover, the present paper discusses the obtained results in relation to present knowledge from both the experimental and theoretical perspectives. Our view is that a consistent picture is now emerging on the structure and relevant optical features (absorption and emission spectra) of these centers. One key aspect of the topic pertains to the generation of self-trapped electrons as small polarons by irradiation of the crystal lattice and their stabilization by oxygen vacancies. What has been learned by observing the interplay between polarons and vacancies has inspired new models for color centers in dielectric crystals, models which represent an advancement from the early models of color centers in alkali halides and simple oxides. The topic discussed in this review is particularly useful to better understand the complex effects of different types of radiation on the defect structure of those materials, therefore providing relevant clues for nuclear engineering applications.

Keywords: lithium niobate; strontium titanate; self-trapped electrons; polarons; oxygen vacancies; defects; luminescence



Citation: Crespillo, M.L.; Graham, J.T.; Agulló-López, F.; Zhang, Y.; Weber, W.J. Real-Time Identification of Oxygen Vacancy Centers in LiNbO_3 and SrTiO_3 during Irradiation with High Energy Particles. *Crystals* **2021**, *11*, 315. <https://doi.org/10.3390/cryst11030315>

Academic Editor: Robert A. Jackson

Received: 8 February 2021

Accepted: 19 March 2021

Published: 22 March 2021

Publisher's Note: MDPI stays neutral with regard to jurisdictional claims in published maps and institutional affiliations.



Copyright: © 2021 by the authors. Licensee MDPI, Basel, Switzerland. This article is an open access article distributed under the terms and conditions of the Creative Commons Attribution (CC BY) license (<https://creativecommons.org/licenses/by/4.0/>).

1. Introduction

Oxides constitute a large family of dielectric compounds that appear in many areas of science and technology from nanoscience to geophysics and from CMOS (Complementary Metal-Oxide-Semiconductor) transistors to astronautics. An important class of oxides are the perovskites, such as cubic strontium titanate (SrTiO_3) and lithium niobate (LiNbO_3), having a distorted perovskite, with a trigonal (ilmenite-like) structure. This later material is a popular example of a photonic material, mainly due to its combination of ferroelectric, photovoltaic, and nonlinear optical properties. In particular, it is the reference material for

second-harmonic generation and more specifically for charge transport (photorefractive) nonlinearities [1]. This latter property has received renewed attention in view of its function in novel applications. For example, LiNbO₃-functionalized surfaces have been used for trapping and manipulating nanoparticles (photovoltaic tweezers) [2]. SrTiO₃ and other cubic perovskites offer outstanding potential for electronic, optoelectronic, and photocatalytic devices and constitute the basis for the new growing field known as complex oxide-based microelectronics [3–7].

This review is mostly concerned with oxygen vacancies in LiNbO₃ and SrTiO₃ as representative examples of distorted and cubic perovskites, although some brief excursions into related materials are occasionally made. The oxygen vacancy centers denoted by F⁺ and F represent an oxygen monovacancy with one trapped electron and an oxygen monovacancy with two trapped electrons, respectively [8]. These two centers are considered to be important point defects for many optical and transport properties and, therefore, for optoelectronic applications of LiNbO₃ and SrTiO₃. We believe that a comparative analysis of these two materials is fruitful and offers a good opportunity to examine, in depth, the role of structure on the properties and behavior of those vacancy defects.

In the basic perovskite ABO₃ structure, A is a monovalent or divalent ion, and B a tetravalent or pentavalent ion. The structure can be described as an arrangement of oxygen BO₆ octahedra, enclosing a transition metal ion B. It is useful to regard those octahedra as the basic structural units governing the electronic and optical behavior. Typical structures for SrTiO₃ and LiNbO₃ crystals are shown in Figure 1, illustrating the different octahedral arrangements. These basic structures allow us to understand many of the basic properties of perovskites. For perovskites, such as SrTiO₃, the oxygen octahedra are linked together at the oxygen vertices. For LiNbO₃, adjacent octahedra share a common face. The occurrence of one or other structure is related to the radii of ions A and B. Indeed, the Goldschmidt tolerance factor, which incorporates the ionic radii, is commonly used to predict the most stable crystal class for a particular perovskite. Note also that several phase transitions have been observed for some of these materials. A key difference between LiNbO₃ and the perovskites is that the ABO₃ phase of LiNbO₃ is stable over a wide range of Li/Nb ratios or stoichiometries. The usual or congruent composition corresponds to [Li]/[Nb] = 0.945, but other stable stoichiometries [9] can be also prepared. A large number of physical properties have been found to depend on stoichiometry, such as the optical absorption edge [10,11] and radiation-excited luminescent emission [12]. A possible reason for the wide range of stable stoichiometries in LiNbO₃ has to do with the close similarities of ionic radii of the host ions (0.68 Å for Li⁺ and 0.69 Å for Nb⁵⁺). In line with the central importance of the structural oxygen octahedra, the electronic band structure of LiNbO₃ [13], SrTiO₃ [14], and other oxide perovskites has some general features. The valence band (VB) is essentially associated with *p*-oxygen orbitals, whereas the conduction band (CB) is constituted by *s*-oxygen orbitals and *d*-orbitals of the B site transition metals. We will see, however, that the *d*-orbitals in the conduction band (CB) also play a key role in our understanding of color centers in oxide perovskites. The band gap, separating the oxygen *p* and *s* orbitals, lies in the range of 3 eV.

The detailed structure of defective crystals in perovskite crystals (particularly LiNbO₃) is a key piece of information to understand most fundamental and functional properties of those materials. However, the generation, identification, and characterization of the defect centers is a difficult subject and involves a complex set of challenges that has been a matter of controversy. A number of works have been dealing with oxygen vacancy models [15–28]. A large variety of experimental techniques have been used to generate and investigate oxygen vacancy centers. Most of these techniques use thermochemical methods (e.g., oxidation reduction treatments) or irradiation with different energetic particles. Thermochemical methods have been employed in LiNbO₃ [15,16], but they rely on subtle thermodynamic models whose parameters are not easy to analyze. Different models have been proposed and discussed to understand the defective structure of reduced LiNbO₃ samples. A very authoritative and elaborated study of those models is given in [29–31].

The defective structure strongly depends on the details of the thermal treatments and the surrounding (reducing) atmosphere and is not the objective of the present work. The major goal of the present work is to focus on the experiments that have been carried out for the production and characterization of oxygen vacancies by high energy particles, either electrons [32,33] or ions [25,26,34].

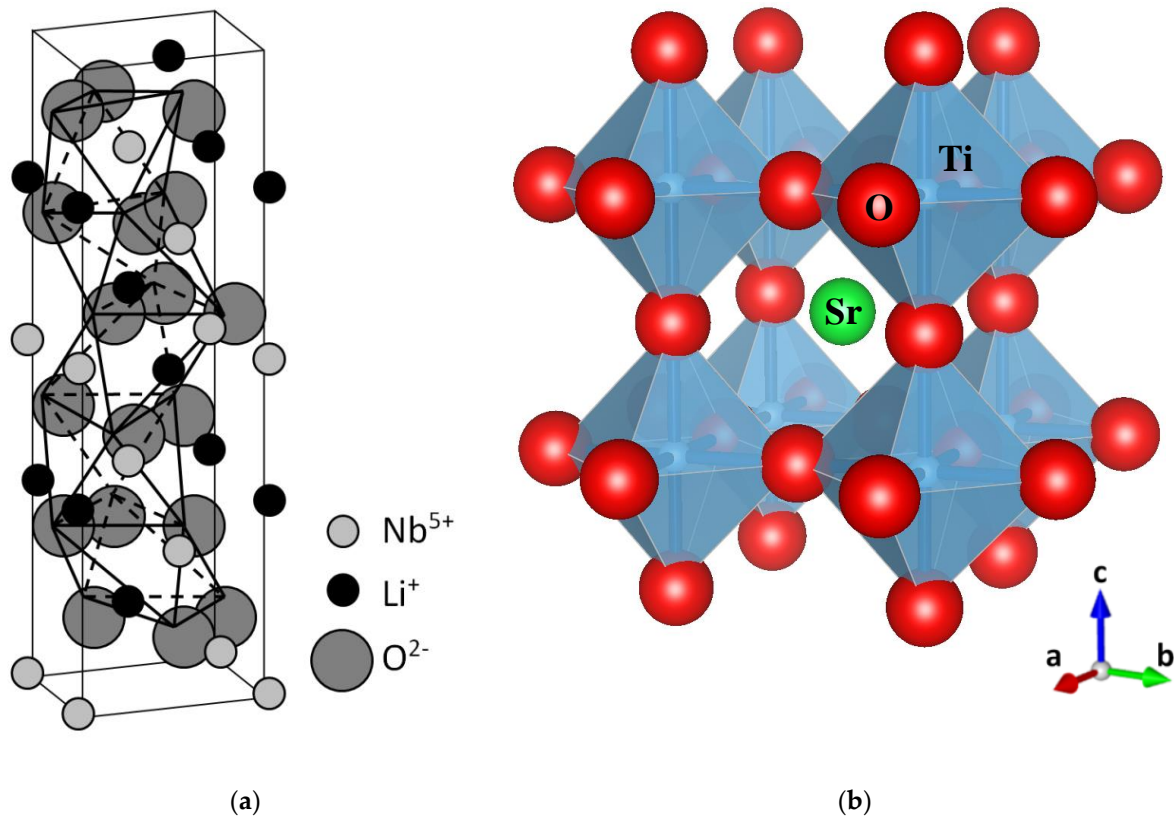


Figure 1. The trigonal ilmenite-like structure of LiNbO_3 (a), and the cubic perovskite structure of SrTiO_3 (b). Schematics show the stacking of oxygen octahedra. In (a), note the tilting (and rotation) of the octahedral units $[\text{NbO}_6]$ along the c -axis. In (b), the $[\text{TiO}_6]$ octahedral units are clearly observed. (a) has been adapted from Xue et al. [35], Copyright (2003), with permission from Elsevier; (b) was generated using Vesta software [36].

These methods rely on the production of atomic displacements induced by momentum transfer during elastic collisions between the fast projectile particles and the atoms of the host crystal lattice. The analysis of these experiments is performed by using well-established models and available software packages [37]. A major experimental advantage of this approach is that the irradiation parameters (energy and range of the particles) can be easily modified and, therefore, the deposited energy and the effects of the damage can be tailored. Although the use of light ions, such as H and He, has been a common tool in the past [38], a growing number of studies has employed swift-heavy ions. This parallels the increased availability of laboratories with swift-heavy ion irradiation capabilities [25,26,34]. Energetic ions have the advantage of producing a broad electronic excitation spectrum that permits simultaneous access to the excited levels of all defect centers. In fact, a relevant outstanding feature of such irradiation experiments is that the production and detection of defects can be performed in situ and in real time. Unfortunately, despite these advantages, the scientific community is often not aware of the potential of the method.

Our review focuses on two representative oxide materials: (a) LiNbO_3 , which is an example of ilmenite-like structure (distorted perovskite), a subject featured in the present issue of *Crystals*, and (b) SrTiO_3 , a technologically important perovskite that is cubic at room temperature (RT), which may serve as an important structure for comparison. In

both cases, significant experimental and theoretical progress has been achieved over the past few years.

The focus of the present review is on the production, optical identification, and electronic structure of oxygen vacancy centers produced by high-energy particles in LiNbO_3 and SrTiO_3 . One important theme is the role of oxygen vacancies assumed as the main traps for electronic carriers through self-trapped electron (polaron) states and the formation of F-type centers. Our understanding of the self-trapping of electronic charges (both electrons and holes) and the further creation of polaron states, predicted by Landau [39], goes back to pioneering works by Schirmer and coworkers on LiNbO_3 [30,40], as well as Stoneham and coworkers in oxides [41,42]. In the case of insulators with high dielectric constants, it is often observed that free electronic carriers self-trap in the perfect lattice due to the induced local polarization, and the subsequent lowering of the energy. Oxygen vacancies and polarons turn out to be closely related and lie at the heart of this discussion. This review examines classic works in the literature, as well as very recent reports, to provide an up-to-date understanding. As a consequence of the extensive work performed on a large variety of oxide perovskites, and the new high-energy irradiation experiments, a satisfactory picture for the structure and optical behavior of oxygen vacancies in these materials is possibly emerging. It is adequate to point out that, at variance with previous investigations, the high-energy irradiation experiments are performed in situ (real-time), avoiding the processes that take place after every irradiation. Therefore, we consider it an opportune moment to present this review centered on the possible generation of oxygen vacancies in LiNbO_3 and SrTiO_3 . It is expected that the comparative discussion between these two representative materials may provide a further impetus for progress in the field.

2. Oxygen Vacancy Centers in LiNbO_3 Created by High-Energy Electron Irradiation: Real Time in situ Detection of the Induced Optical Absorption

LiNbO_3 is a reference inorganic material for nonlinear optical applications, particularly in relation to charge transport (photorefractive) nonlinearities. The experiments to be discussed here involve the measurement of the optical absorption spectra induced by high-energy electron irradiation up to 2 MeV on congruent samples [32]. In these pioneer experiments, a sample is sandwiched inside a small double oven situated in a vacuum irradiation chamber, which allows for enabling in situ measurement of the optical absorption spectrum in real time. For low-electron energies, a low intensity, broad, and structureless absorption spectrum is produced. However, for higher energies (>0.3 MeV), a more well-defined absorption spectrum develops with a broad peak at about 2.6 eV (480 nm). The spectrum has been now decomposed into three main Gaussian components centered at 1.7, 2.6, and 3.2 eV, as illustrated in Figure 2. The component at 1.7 eV (730 nm) was previously associated with mobile small electron polarons such as Nb^{4+} [40] through electron spin resonance (ESR) measurements after X-ray irradiation at 20 K, and has been also detected in thermally reduced samples [15,16]. These self-trapped carriers such as Nb^{4+} constitute a localized electronic defect that can migrate through the lattice by hopping between nearby lattice sites [43]. In order to investigate the structural origin of the absorption band centered at 2.6 eV, researchers plotted its height as a function of the electron beam energy (see reference for further details). The optical density as a function of electron irradiation showed a threshold at an energy of 1.1 MeV (Figure 3); thus, in addition to the energy loss in 0.9 mm, a threshold value of 0.3 MeV can be deduced (more details can be found elsewhere [32]). Considering the energy transfer between the high-energy electrons and the LiNbO_3 lattice, the sharp threshold was associated with displacement of oxygen atoms by elastic electron–atom collisions. The oxygen displacement energy was determined to be 53 eV, which is similar to the values found for other oxides such as MgO (60 eV), MgAl_2O_4 (59 eV), and Al_2O_3 (70 eV). It is worth noting that similar absorption spectra have also been obtained after thermal reduction [15,16] where the generation of oxygen vacancies has not been demonstrated and alternative models have been invoked [29,30,44]. Pending of ESR experiments and refined theoretical calculations, a main tentative conclusion is that electron irradiation experiments can provide clear and unequivocal evidence for the

generation and optical behavior of oxygen vacancy centers, i.e., F^+ and F centers. Similar irradiation experiments to those reported on congruent samples were also carried out on stoichiometric samples ($Li/Nb = 1$) [33]. The generated absorption spectrum is similar in both cases, indicating that it is essentially independent of the structure associated with the non-stoichiometry.

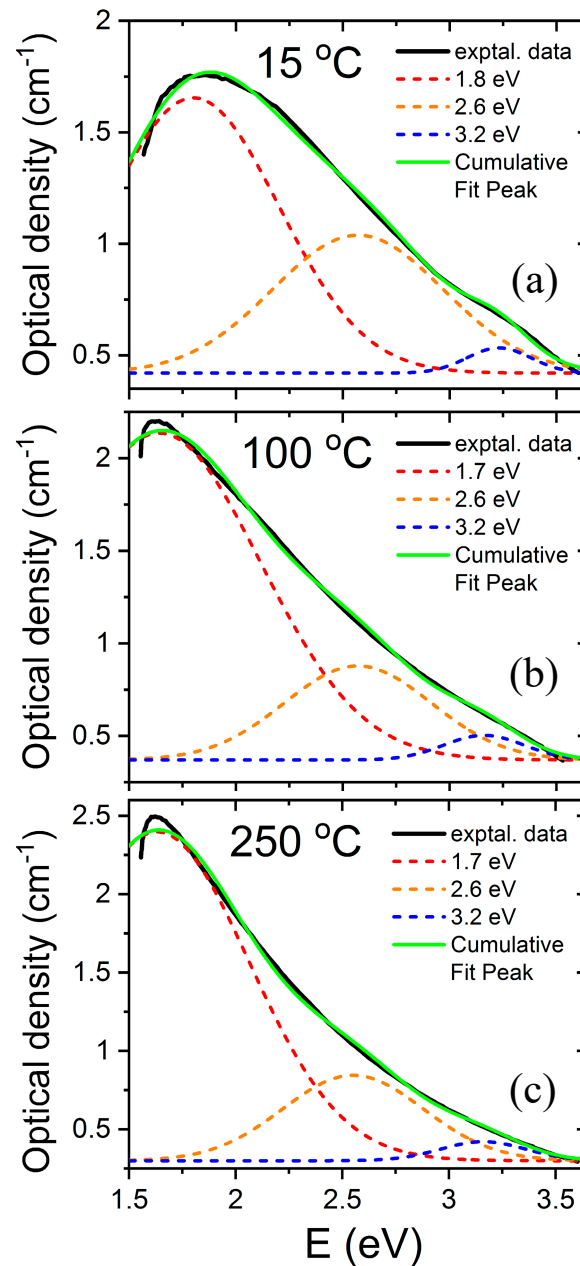


Figure 2. Absorption spectra and Gaussian decomposition obtained for congruent $LiNbO_3$ irradiated with high-energy electrons at various temperatures (a) 15 °C, (b) 100 °C, (c) 250 °C. This figure has been adapted from Hodgson et al. [32], Copyright (1987), with permission from Elsevier.

In the light of the available information presented in the section on $SrTiO_3$ as well as on other perovskites, one could associate the measured absorption bands to one or two Nb^{4+} small polarons trapped at the vacancy site, respectively. This model is rather different from the earlier one used to describe color centers in alkali halides, where the electrons are deeply trapped in vacancies. This is the model described in the next section on high-energy, ion-irradiated $SrTiO_3$. In order to explore the validity of such interpretation for F -type

centers in LiNbO₃, researchers performed complementary experiments to observe the effect of heating on the absorption spectra (Figure 4). It was shown that heating in the range RT–250 °C caused a clear conversion of the 2.6 eV band into the 1.7 eV band. This behavior was reversible on cooling the samples. It was, then, concluded that F⁺-centers (one electron trapped at the vacancy) and F-centers (two electrons trapped at the vacancy) might be reasonable candidates for the 3.2 eV and 2.6 eV bands, respectively. The process can be summarized as follows. With the addition of thermal activation energy, the Nb⁴⁺ polarons became untrapped from the vacancy sites, giving rise to its 1.7 eV band and causing the F to F⁺ conversion and the generation of free oxygen vacancies. The behavior was essentially reversible on cooling, clearly suggesting that the polarons trapped again at the vacancies. In other words, vacancies and polarons should stay close together so that the balance between the centers at 1.7 eV and 2.6 eV and the generated concentration of vacancies appear to be essentially governed by thermodynamic laws. The optical absorption bands of the F-type color centers would involve the transition between an in-gap ground state to excited Nb⁴⁺ *d*-levels residing in the conduction band (CB) [17]. Although, ESR experiments and theoretical calculations have yet to corroborate this model, the available data suggest that these color centers involve small Nb⁴⁺ polarons that are trapped in the vicinity of oxygen vacancies and form part of their electronic structure. Anyhow, one should point out that alternative models for the optical absorption spectra of the irradiated (as well as reduced) crystals have been discussed in terms of polaron and bipolaron states [30].

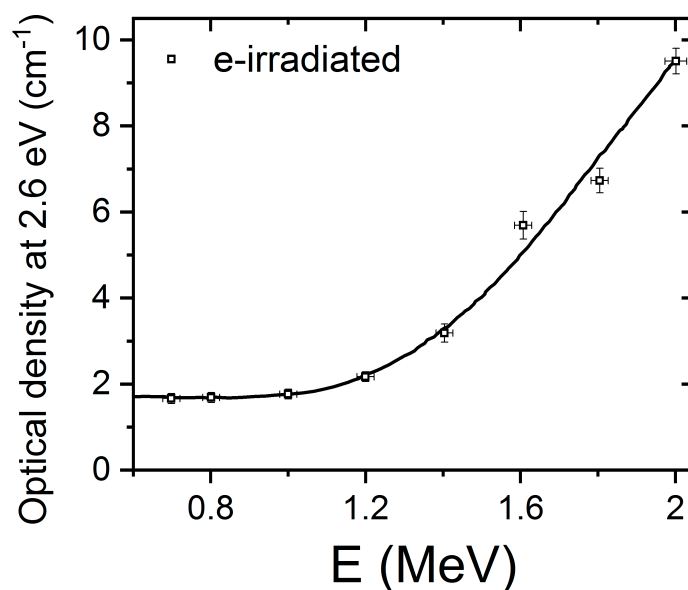


Figure 3. Normalized height of the optical absorption band at 2.6 eV as a function of the electron beam energy for congruent LiNbO₃. This figure has been adapted from Hodgson et al. [32], Copyright (1987), with permission from Elsevier.

It is encouraging to note that similar high-energy electron irradiation experiments have been also carried out on KNbO₃ (a cubic/orthorhombic perovskite) [45]. The absorption spectra are qualitatively and quantitatively similar to those obtained for LiNbO₃, confirming the key role of the NbO₆ octahedron in the optical response. Moreover, the experimental data also show a sharp threshold in optical density as a function of the electron energy in accordance with the impact character of the process. In our view, all these results demonstrate the potential of high-energy electron irradiation experiments to introduce oxygen vacancies in a reliable way and allow for their real-time characterization. These results could not be, in principle, achieved by any alternative methods.

At this stage, one may ask about the possible luminescence emissions associated with those color centers in LiNbO₃. They might provide additional insights on the responsible

optical transitions, as well as on the electronic energy levels. Early luminescence experiments under X-ray irradiation showed a main emission band at around 2.9 eV, but it was found to be independent of irradiation dose [46]. Therefore, this emission was not ascribed to oxygen vacancies or any extrinsic defects, but to intrinsic electron–hole (e - h) recombination. The reason may lie in the fact that, after generation of free electrons (e) and holes (h) by irradiation, those pairs very rapidly couple together and form relaxed self-trapped excitons (STEs) on the sub-nanosecond time scale. Moreover, the fraction of these STEs appears to be very high (close to 1), and thus this recombination channel appears dominant.

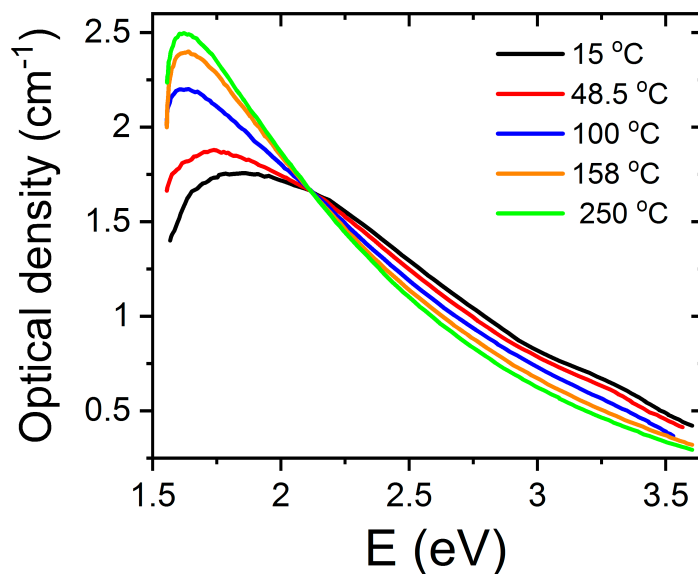


Figure 4. Effect of heating/cooling on the absorption spectra of congruent LiNbO₃ irradiated with high-energy electrons. This figure has been adapted from Hodgson et al. [32], Copyright (1987), with permission from Elsevier.

3. Oxygen Vacancy Centers in Cubic SrTiO₃ under High-Energy Ion Beam Irradiation: Real-Time Luminescence Emissions

A large fraction of the recent reports on oxide perovskites is related to SrTiO₃ [28], where the recent experimental and theoretical information has improved our understanding of the structure and behavior of oxygen vacancies. They are considered to be responsible for some outstanding properties of SrTiO₃ such as an insulating metal transition, superconductive behavior, and photocatalytic properties [3,47]. Therefore, in line with the objectives of this review, we now discuss recent experimental data obtained from irradiation experiments on SrTiO₃ using high-energy heavy-ion beams [25,26,48]. The use of such ions has dramatically increased in recent years. For high-energy, high-mass ions, the electronic stopping power is large and dominates the total stopping power. This large electronic stopping power gives rise to specific types of lattice damage and amorphization [34,49]. In contrast with the experiments in LiNbO₃ discussed in a previous section, which relied on absorbance spectra, the main detection technique with the heavy ion experiments has been luminescence. One should note that ion beam induced luminescence or ionoluminescence experiments are unique in their ability to combine high sensitivity with high spectral resolution. In such a way, the experiments offer a complementary picture to those ones described previously in Section 2 for LiNbO₃ and offer an experimental approach for the future.

The light emission spectra of SrTiO₃ under ion beam irradiation is complex and includes several overlapping bands, as shown in Figure 5, with peaks located at around 2.0, 2.5, and 2.8 eV [25–27,48]. Their relative importance strongly depends on the mass and energy of the projectile ions, which determines the electronic excitation density deposited

into the material, as well as on the irradiation temperature. Moreover, heavy ions, may also introduce structural defects within the material. While these additional variables can complicate the interpretation, they also act as useful knobs to turn that allow the experimenter to gain insight into the nature of the luminescence centers. Recently, a detailed study of the luminescence emission under irradiation with a variety of high-energy heavy ions has provided unequivocal evidence supporting the assignment of the 2.0 eV emission band to Ti^{3+} polarons trapped at isolated oxygen vacancies [25,26]. In fact, the data in Figure 6 show a strong correlation between the initial growth rate of the 2.0 eV band and the production rate of isolated vacancies with irradiation fluence, as calculated by SRIM (The Stopping and Range of Ions in Matter) simulation code [37]. Density functional theory (DFT) calculations [50] indicate that the corresponding luminescence transition connects an in-gap level, having a d -orbital character, to Ti^{3+} d -levels located in the conduction band (CB). Note the similarity of this transition to the in-gap d -orbital to CB d -orbital Nb^{4+} transition associated with F-centers in electron irradiated LiNbO_3 . One should note that X-ray irradiation of SrTiO_3 , which does not cause lattice damage by impact collisions, does not induce the red emission associated to the proposed oxygen vacancies [51]. A schematic of the electronic structure of the oxygen vacancy center is depicted in Figure 7. The 2.0 eV band has not been often observed with pulsed laser excitation partly due to the difficulty of reaching the upper d -levels in the conduction band (CB) with a narrow spectral width excitation source. Other theoretical calculations have dealt with this complex problem [23,52,53], and aside from the technical details, they seem to lend support to the argument that F-type centers are small Ti^{3+} electron polarons trapped at oxygen vacancies.

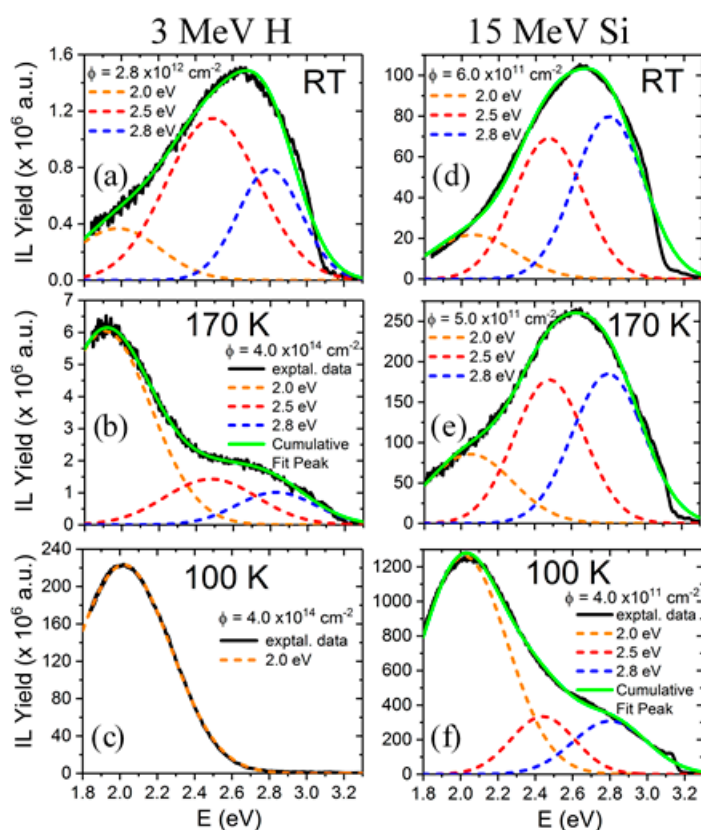


Figure 5. Luminescence emission spectra and Gaussian band components (centered at 2.0, 2.5, and 2.8 eV) of SrTiO_3 obtained under irradiation with several high-energy projectile ions and energies at several temperatures (100 K, 170 K and RT, see labels). Irradiation with 3 MeV H (a–c) and 15 MeV Si (d–f) ions have been selected to show the complexity of overlapping emission bands. This figure has been adapted from Crespillo et al. [27].

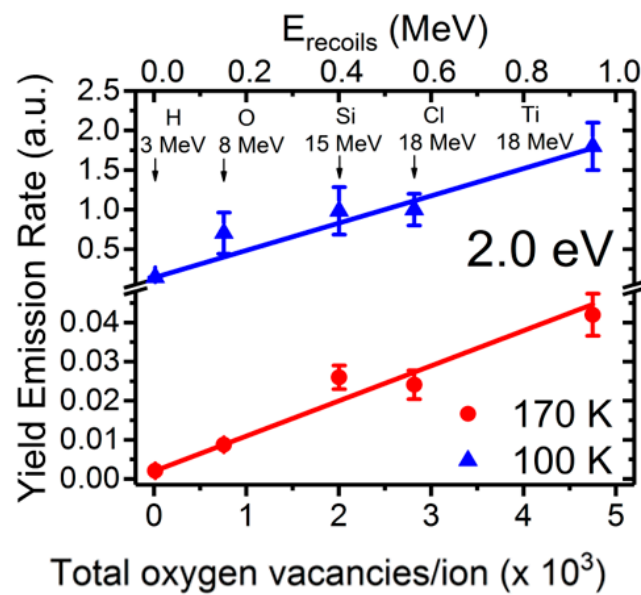


Figure 6. Normalized initial growth rate of the 2.0 eV emission band in SrTiO₃, associated with isolated oxygen vacancies, as a function of the vacancy production rate calculated by the SRIM code [37] under irradiation with several high-energy ions and energies (see labels). A clear linear correlation is observed for all the ions at both temperatures. This figure has been adapted from Crespillo et al. [25], Copyright (2018), with permission from Elsevier.

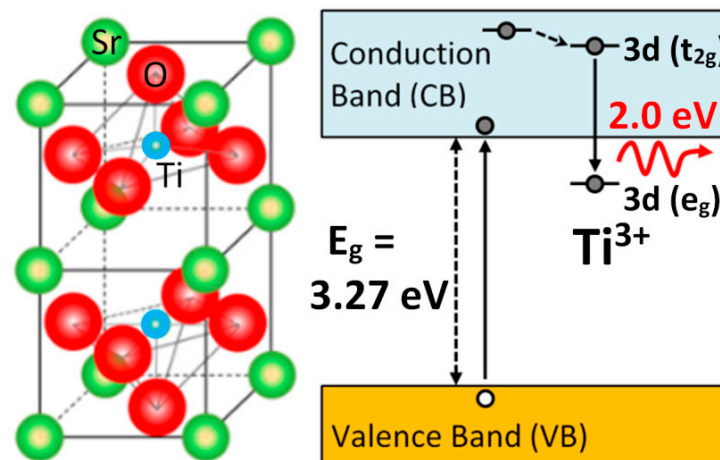


Figure 7. Schematics of the structure and electronic levels for the oxygen vacancy centers in SrTiO₃. Possible mechanisms of the electronic processes involving the electron polaron (Ti³⁺) trapped adjacent to oxygen vacancies. The transition inside the TiO₆ octahedron involving the excited (t_{2g}) and ground (e_g) levels gives rise to the 2.0 eV red luminescence band. This figure has been adapted from Crespillo et al. [25], Copyright (2018), with permission of Elsevier.

Unfortunately, ESR measurements have not yet been able to provide a detailed map for the electronic structure of the oxygen vacancy centers. Nevertheless, it may be useful to comment on the detection by ESR of Ta⁴⁺-polarons in KTaO₃ as a consequence of light irradiation with energies close to, but above, the band gap [19]. Various Ta centers have been identified and associated with oxygen vacancies. These centers break the cubic symmetry and behave as symmetry-breaking defects that are able to induce a local polar cluster at low enough temperatures (<50 K). They are responsible for second-harmonic generation (SHG) and first-order Raman scattering, among other effects. Consequently, the model derived from the ESR data indicates that the Ta⁴⁺ centers are located on ions nearest to the oxygen vacancy. We expect a similar defect structure in SrTiO₃ and LiNbO₃.

The centers behave as shallow electron donors with ground state energy levels close to the bottom of the conduction band (CB), around 26 meV.

4. Summary and Conclusions

From the results discussed in this review, detailed optical information has been obtained, which may contribute to understanding of the occurrence and behavior of oxygen vacancy centers in distorted (LiNbO₃) and cubic (SrTiO₃) perovskites. Irradiations with high-energy particles have provided real-time in situ information about their optical features. In particular, absorption bands in LiNbO₃ (1.7, 2.6, and 3.2 eV) and luminescence emissions (2.0 eV) in SrTiO₃ have been obtained under electron and ion beam irradiation, respectively. These spectral features can be used for the identification of the responsible centers and for monitoring their evolution and kinetics. It is important to mention that using these in situ techniques, it is possible to increase the concentration of structural defects and simultaneously monitor the optical response, thereby allowing the experimenter to associate optical spectra with lattice defect centers.

These techniques lend evidence that electrons are trapped as small polarons at host cation sites close to oxygen vacancies, although additional work is still needed. The absorption and emission bands have been ascribed to optical transitions between in-gap levels and levels within the conduction band (CB) associated with the polaron (transition metal) states. The joint analysis of these experiments together with available theoretical calculations has helped form a reasonable (although incomplete) picture of the electronic structure for oxygen vacancy centers in oxide perovskites. For LiNbO₃, the experimental data on high-energy electron irradiations have shown a link between the displacement of oxygen atoms and the occurrence of these optical transitions, confirming that oxygen vacancies act as efficient traps for small polarons. There are still a number of pending problems to be solved, such as determining the precise location of the corresponding electronic energy levels within the bandgap. This is not an easy task due to the many body nature of the phenomena and the need to simultaneously characterize and understand structural disorder and carrier dynamics. A specific feature to LiNbO₃ is the role that stoichiometry plays. The wide range of Li/Nb ratios would add an additional variable to the problem. Nevertheless, the relative insensitivity of the optical behavior to that ratio seems to reinforce the conclusion that the main electronic and optical behavior of ABO₃ perovskites is dominated by the basic octahedral BO₆ units.

As to future trends in the field, one should remark that the surfaces of perovskites have a great and largely unexplored potential, particularly LiNbO₃. In the area of functional materials, the surface of LiNbO₃ is a fertile area. Better knowledge of the surface structure and its properties (including oxygen vacancies) [22,52] would offer the possibility of nanoscale devices, molecular detection, and efficient catalysts [54], among other applications. This remark is of special relevance in relation to real-time operation of optoelectronic (photovoltaic) tweezers in LiNbO₃ and will advance our understanding of the trapping and untrapping cycles during their operation [55]. Furthermore, recent publications can be found in the literature showing potential applications in neuromorphic computing through the production of oxygen vacancies in LiNbO₃ thin films by Ar⁺ irradiation [56].

Funding: This work has been supported by the U.S. Department of Energy, Office of Science, Basic Energy Sciences, Materials Sciences and Engineering Division under Contract DE-AC05-00OR22725. M.L.C. acknowledges support from the University of Tennessee Governor's Chair program.

Acknowledgments: The authors would like to pay special tribute to the pioneering role played by our colleague Ortwin Schirmer, who is responsible for many of the key achievements in the field. In particular, we deeply acknowledge and appreciate the illuminating comments and discussions we had with him in relation to some of the works cited in this review.

Conflicts of Interest: The authors declare no conflict of interest.

References

1. Günter, P.; Huignard, J.P. *Photorefractive Materials and Their Applications 1: Basic Effects*; Springer: New York, NY, USA, 2006.
2. García-Cabañes, A.; Blázquez-Castro, A.; Arizmendi, L.; Agulló-López, F.; Carrascosa, M. Recent Achievements on Photovoltaic Optoelectronic Tweezers Based on Lithium Niobate. *Crystals* **2018**, *8*, 65. [[CrossRef](#)]
3. Ogale, S.B. *Thin Films and Heterostructures for Oxide Electronics*; Springer: New York, NY, USA, 2005.
4. Reyren, N.; Thiel, S.; Caviglia, A.; Kourkoutis, L.F.; Hammerl, G.; Richter, C.; Schneider, C.W.; Kopp, T.; Ruetschi, A.-S.; Jaccard, D.; et al. Superconducting Interfaces Between Insulating Oxides. *Science* **2007**, *317*, 1196–1199. [[CrossRef](#)] [[PubMed](#)]
5. Brinkman, A.; Huijben, M.; Van Zalk, M.; Zeitler, U.; Maan, J.C.; Van Der Wiel, W.G.; Rijnders, G.; Blank, D.H.A.; Hilgenkamp, H. Magnetic effects at the interface between non-magnetic oxides. *Nat. Mater.* **2007**, *6*, 493–496. [[CrossRef](#)] [[PubMed](#)]
6. Wang, D.; Ye, J.; Kako, T.; Kimura, T. Photophysical and Photocatalytic Properties of SrTiO₃ Doped with Cr Cations on Different Sites. *J. Phys. Chem. B* **2006**, *110*, 15824–15830. [[CrossRef](#)]
7. Crespillo, M.L.; Graham, J.T.; Agulló-López, F.; Zhang, Y.; Weber, W.J. Correlation between Cr³⁺ Luminescence and Oxygen Vacancy Disorder in Strontium Titanate under MeV Ion Irradiation. *J. Phys. Chem. C* **2017**, *121*, 19758–19766. [[CrossRef](#)]
8. Agulló-López, F.; Catlow, C.R.; Townsend, P.D. *Point Defects in Materials*; Academic Press: London, UK, 1984.
9. Polgár, K.; Péter, Á.; Kovacs, L.; Corradi, G.; Szaller, Z. Growth of stoichiometric LiNbO₃ single crystals by top seeded solution growth method. *J. Cryst. Growth* **1997**, *177*, 211–216. [[CrossRef](#)]
10. Kovacs, L.; Ruschhaupt, G.; Polgár, K.; Corradi, G.; Wohlecke, M. Composition dependence of the ultraviolet absorption edge in lithium niobate. *Appl. Phys. Lett.* **1997**, *70*, 2801–2803. [[CrossRef](#)]
11. Krol, D.M.; Blasse, G.; Powell, R.C. The influence of the Li/Nb ratio on the luminescence properties of LiNbO₃. *J. Chem. Phys.* **1980**, *73*, 163. [[CrossRef](#)]
12. García-Cabañes, A.; Sanz-García, J.A.; Cabrera, J.M.; Agulló-López, F.; Zaldo, C.; Pareja, R.; Polgár, K.; Raksányi, K.; Fölvári, I. Influence of stoichiometry on defect-related phenomena in LiNbO₃. *Phys. Rev. B* **1988**, *37*, 6085–6091. [[CrossRef](#)]
13. Javid, M.A.; Khan, Z.U.; Mehmood, Z.; Nabi, A.; Hussain, F.; Imran, M.; Nadeem, M.; Anjum, N. Structural, electronic and optical properties of LiNbO₃ using GGA-PBE and TB-mBJ functionals: A DFT study. *Int. J. Mod. Phys. B* **2018**, *32*, 1850168. [[CrossRef](#)]
14. Van Benthem, K.; Elsässer, C.; French, R.H. Bulk electronic structure of SrTiO₃: Experiment and theory. *J. Appl. Phys.* **2001**, *90*, 6156–6164. [[CrossRef](#)]
15. Sweeney, K.L.; Halliburton, L.E. Oxygen vacancies in lithium niobate. *Appl. Phys. Lett.* **1983**, *43*, 336–338. [[CrossRef](#)]
16. García-Cabañes, A.; Dieguez, E.; Cabrera, J.M.; Agulló-López, F. Contributing bands to the optical absorption of reduced LiNbO₃: Thermal and optical excitation. *J. Phys. Condens. Mat.* **1989**, *1*, 6453–6462. [[CrossRef](#)]
17. DeLeo, G.G.; Dobson, J.L.; Masters, M.F.; Bonjack, L.H. Electronic structure of an oxygen vacancy in lithium niobate. *Phys. Rev. B* **1988**, *37*, 8394–8400. [[CrossRef](#)] [[PubMed](#)]
18. Kotomin, E.A.; Eglitis, R.I.; Popov, A.I. Charge distribution and optical properties of and F centres in crystals. *J. Phys. Condens. Mat.* **1997**, *9*, L315–L321. [[CrossRef](#)]
19. Laguta, V.V.; Zaritskii, M.I.; Glinchuk, M.D.; Bykov, I.P.; Rosa, J.; Jastrabík, L. Symmetry-breaking Ta⁴⁺ centers in KTaO₃. *Phys. Rev. B* **1998**, *58*, 156–163. [[CrossRef](#)]
20. Meldrum, A.; Boatner, L.; Ewing, R. Effects of ionizing and displacive irradiation on several perovskite-structure oxides. *Nucl. Instrum. Methods Phys. Res. Sect. B* **1998**, *141*, 347–352. [[CrossRef](#)]
21. Eglitis, R.; Kotomin, E.; Borstel, G. Quantum chemical modelling of “green” luminescence in ABO₃ perovskites. *Eur. Phys. J. B* **2002**, *27*, 483–486. [[CrossRef](#)]
22. Zhukovskii, Y.F.; Kotomin, E.A.; Evarestov, R.A.; Ellis, D.E. Periodic models in quantum chemical simulations of F centers in crystalline metal oxides. *Int. J. Quantum Chem.* **2007**, *107*, 2956–2985. [[CrossRef](#)]
23. Janotti, A.; Varley, J.B.; Choi, M.; Van De Walle, C.G. Vacancies and small polarons in SrTiO₃. *Phys. Rev. B* **2014**, *90*, 085202. [[CrossRef](#)]
24. Wang, C.; Sun, J.; Ni, W.; Yue, B.; Hong, F.; Liu, H.; Cheng, Z. Tuning oxygen vacancy in LiNbO₃ single crystals for prominent memristive and dielectric behaviors. *J. Am. Ceram. Soc.* **2019**, *102*, 6705–6712. [[CrossRef](#)]
25. Crespillo, M.; Graham, J.; Agulló-López, F.; Zhang, Y.; Weber, W. Isolated oxygen vacancies in strontium titanate shine red: Optical identification of Ti³⁺ polarons. *Appl. Mater. Today* **2018**, *12*, 131–137. [[CrossRef](#)]
26. Crespillo, M.L.; Graham, J.; Agulló-López, F.; Zhang, Y.; Weber, W. Role of oxygen vacancies on light emission mechanisms in SrTiO₃ induced by high-energy particles. *J. Phys. D Appl. Phys.* **2017**, *50*, 155303. [[CrossRef](#)]
27. Crespillo, M.L.; Graham, J.T.; Agulló-López, F.; Zhang, Y.; Weber, W.J. The blue emission at 2.8 eV in strontium titanate: Evidence for a radiative transition of self-trapped excitons from unbound states. *Mater. Res. Lett.* **2019**, *7*, 298–303. [[CrossRef](#)]
28. Crespillo, M.L.; Graham, J.T.; Agulló-López, F.; Zhang, Y.; Weber, W.J. Recent Advances on Carrier and Exciton Self-Trapping in Strontium Titanate: Understanding the Luminescence Emissions. *Crystals* **2019**, *9*, 95. [[CrossRef](#)]
29. Schirmer, O.F.; Reyher, H.-J.; Wöhlecke, M. Characterization of point defects in photorefractive oxide crystals by para-magnetic resonance methods. In *Insulating Materials for Optoelectronics: New Developments*; Agulló-López, F., Ed.; World Scientific: London, UK, 1995; pp. 93–124.
30. Schirmer, O.F.; Imlau, M.; Merschjann, C.; Schoke, B. Electron small polarons and bipolarons in LiNbO₃. *J. Phys. Condens. Matter* **2009**, *21*, 123201. [[CrossRef](#)]

31. Halliburton, L.; Sweeney, K.; Chen, C. Electron spin resonance and optical studies of point defects in lithium niobate. *Nucl. Instrum. Methods Phys. Res. Sect. B* **1984**, *1*, 344–347. [[CrossRef](#)]
32. Hodgson, E.; Agulló-López, F. Oxygen vacancy centres induced by electron irradiation in LiNbO₃. *Solid State Commun.* **1987**, *64*, 965–968. [[CrossRef](#)]
33. Hodgson, E.R.; Agullo-Lopez, F. High-energy electron irradiation of stoichiometric LiNbO₃. *J. Phys. Condens. Matter* **1989**, *1*, 10015–10020. [[CrossRef](#)]
34. Agulló-López, F.; Climent-Font, A.; Muñoz-Martín, Á.; Olivares, J.; Zucchiatti, A. Ion beam modification of dielectric materials in the electronic excitation regime: Cumulative and exciton models. *Prog. Mater. Sci.* **2016**, *76*, 1–58. [[CrossRef](#)]
35. Xue, D.; Kitamura, K.; Wang, J. Atomic packing and octahedral linking model of lithium niobate single crystals. *Opt. Mater.* **2003**, *23*, 399–402. [[CrossRef](#)]
36. Momma, K.; Izumi, F. VESTA 3 for three-dimensional visualization of crystal, volumetric and morphology data. *J. Appl. Crystallogr.* **2011**, *44*, 1272–1276. [[CrossRef](#)]
37. Ziegler, J.F.; Ziegler, M.; Biersack, J. SRIM—The stopping and range of ions in matter (2010). *Nucl. Instrum. Methods Phys. Res. Sect. B* **2010**, *268*, 1818–1823. [[CrossRef](#)]
38. Townsend, P.D.; Chandler, P.J.; Zhang, L. *Optical Effects of Ion Implantation (Cambridge Studies in Modern Optics)*; Cambridge University Press: Cambridge, UK, 1996.
39. Landau, L.D. Über die Bewegung der Elektronen im Kristallgitter. *Phys. Zeit. Sowjetunion* **1933**, *3*, 664–665.
40. Schirmer, O.F.; Von Der Linde, D. Two-photon- and x-ray-induced Nb⁴⁺ and O—small polarons in LiNbO₃. *Appl. Phys. Lett.* **1978**, *33*, 35–38. [[CrossRef](#)]
41. Stoneham, A.; Itoh, N. Materials modification by electronic excitation. *Appl. Surf. Sci.* **2000**, *168*, 186–193. [[CrossRef](#)]
42. Stoneham, A.M.; Gavartin, J.; Shluger, A.L.; Kimmel, A.V.; Ramo, D.M.; Rønnow, H.M.; Aeppli, G.; Renner, C. Trapping, self-trapping and the polaron family. *J. Phys. Condens. Matter* **2007**, *19*, 255208. [[CrossRef](#)]
43. Sturman, B.; Carrascosa, M.; Agullo-Lopez, F. Light-induced charge transport in LiNbO₃ crystals. *Phys. Rev. B* **2008**, *78*, 245114. [[CrossRef](#)]
44. Lengyel, K.; Péter, Á.; Kovacs, L.; Corradi, G.; Palfalvi, L.; Hebling, J.; Unferdorben, M.; Dravecz, G.; Hajdara, I.; Szaller, Z.; et al. Growth, defect structure, and THz application of stoichiometric lithium niobate. *Appl. Phys. Rev.* **2015**, *2*, 040601. [[CrossRef](#)]
45. Hodgson, E.; Zaldo, C.; Agulló-López, F. Atomic displacement damage in electron irradiated KNbO₃. *Solid State Commun.* **1990**, *75*, 351–353. [[CrossRef](#)]
46. Arizmendi, L.; Cabrera, J.; Agulló-López, F. X-ray induced luminescence of LiNbO₃. *Solid State Commun.* **1981**, *40*, 583–585. [[CrossRef](#)]
47. Harrigan, W.L.; Michaud, S.E.; Lehuta, K.A.; Kittilstved, K.R. Tunable Electronic Structure and Surface Defects in Chromium-Doped Colloidal SrTiO₃– δ Nanocrystals. *Chem. Mater.* **2016**, *28*, 430–433. [[CrossRef](#)]
48. Kan, D.; Terashima, T.; Kanda, R.; Masuno, A.; Tanaka, K.; Chu, S.; Kan, H.; Ishizumi, A.; Kanemitsu, Y.; Shimakawa, Y.; et al. Blue-light emission at room temperature from Ar⁺-irradiated SrTiO₃. *Nat. Mater.* **2005**, *4*, 816–819. [[CrossRef](#)]
49. Zhang, Y.; Weber, W.J. Ion irradiation and modification: The role of coupled electronic and nuclear energy dissipation and subsequent nonequilibrium processes in materials. *Appl. Phys. Rev.* **2020**, *7*, 041307. [[CrossRef](#)]
50. Ricci, D.; Bano, G.; Pacchioni, G.; Illas, F. Electronic structure of a neutral oxygen vacancy in SrTiO₃. *Phys. Rev. B* **2003**, *68*, 224105. [[CrossRef](#)]
51. Aguilar, M. X-ray induced processes in SrTiO₃. *J. Appl. Phys.* **1982**, *53*, 9009. [[CrossRef](#)]
52. Alexandrov, V.E.; Kotomin, E.A.; Maier, J.; Evarestov, R.A. First-principles study of bulk and surface oxygen vacancies in SrTiO₃ crystal. *Eur. Phys. J. B* **2009**, *72*, 53–57. [[CrossRef](#)]
53. Mitra, C.; Lin, C.; Robertson, J.; Demkov, A.A. Electronic structure of oxygen vacancies in SrTiO₃ and LaAlO₃. *Phys. Rev. B* **2012**, *86*, 155105. [[CrossRef](#)]
54. Sanna, S.; Schmidt, W.G. LiNbO₃ surfaces from a microscopic perspective. *J. Phys. Condens. Matter* **2017**, *29*, 413001. [[CrossRef](#)]
55. Sebastián-Vicente, C.; Muñoz-Cortés, E.; García-Cabañes, A.; Agulló-López, F.; Carrascosa, M. Real-Time Operation of Photo-voltaic Optoelectronic Tweezers: New Strategies for Massive Nano-object Manipulation and Reconfigurable Patterning. *Part. Part. Syst. Character.* **2019**, *36*, 1900233. [[CrossRef](#)]
56. Pan, X.; Shuai, Y.; Wu, C.; Zhang, L.; Guo, H.; Cheng, H.; Peng, Y.; Qiao, S.; Luo, W.; Wang, T.; et al. Ar⁺ ions irradiation induced memristive behavior and neuromorphic computing in monolithic LiNbO₃ thin films. *Appl. Surf. Sci.* **2019**, *484*, 751–758. [[CrossRef](#)]